Notes

Effect of Edge Fracture on Constant Torque Rheometry of Entangled Polymer Solutions

Yong Woo Inn,† Kurt F. Wissbrun, and Morton M. Denn*

Benjamin Levich Institute for Physico-Chemical Hydrodynamics, City College of New York, CUNY, New York, New York 10031

Received May 27, 2005
Revised Manuscript Received July 14, 2005

1. Introduction

Tapadia and Wang[1,2] have recently reported a discontinuity in the flow curve of a highly entangled 10% solution of 1,4-polybutadiene dissolved in oligomeric butadiene. They attribute the discontinuity to an "entanglement−disentanglement transition" (EDT), which they contend is "a great challenge for existing constitutive models". The discontinuity was observed in a torque-controlled rheometer (usually called a stress-controlled rheometer) but not in a displacement-controlled rheometer. We have repeated Tapadia and Wang's experiments in a torque-controlled rheometer and have obtained completely analogous results. We can account fully for the shapes of the observed flow curves, however, by the occurrence of edge fracture, which results in loss of material from the test fixture and consequent increase of shear rate while shearing at a controlled torque.

We have carried out experiments on two solutions. The first was a 10 wt % solution of 1,4-polybutadiene (Polymer Source Inc., $M_w = 1.24 \times 10^6$ g/mol, $M_w/M_n = 1.13$) dissolved in phenyl-terminated oligomeric butadiene (Aldrich, $M_n \sim 1500$ g/mol); this is the system studied by Tapadia and Wang, although the polymer was probably from a different batch, since they reported a polydispersity of 1.2. The second was a 7.5 wt % solution of 1,4-polybutadiene in phenyl-terminated oligomeric butadiene. This sample was kindly provided by Professor Wang, who indicated that the 7.5% solution was similar in behavior to the 10% solution studied by Tapadia and Wang and was more appropriate for use in the rheometer fixture that we planned to use. It is our understanding that this polymer is from Goodyear Tire and Rubber, with $M_w = 1.75 \times 10^6$ g/mol, $M_w/M_n = 1.34$. Experiments were performed at 30 °C in an AR1000 torque-controlled rheometer (TA Instruments) using a 40 mm diameter cone-and-plate fixture with a 2° cone angle.

2. 10% Solution

Figure 1 shows the results of creep experiments at constant nominal stresses ranging from 500 to 4500 Pa,

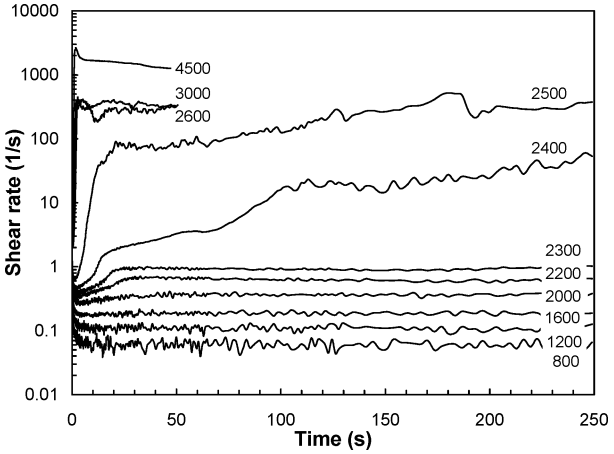

Figure 1. Shear rates as functions of time at constant input stresses from 500 to 4500 Pa for the 10% sample. The sample was fully relaxed for 5 min after each creep experiment and then stepped up to the next stress.

which should be compared to Figure 6a in Tapadia and Wang.[1] The sample was permitted to relax without stress for 5 min after each measurement and then stepped up to the designated stress, starting at 500 Pa and increasing to 4500 Pa. The shape change between 2300 and 2500 Pa, with an increase in shear rate of 2 orders of magnitude, and the long, slow transient at 2400 Pa, with an apparent shoulder between about 10 and 70 s, are the same as the transition observed by Tapadia and Wang between 2000 and 3000 Pa and their transient at 2500 Pa. This transient is the signature of their proposed "EDT". The long transient in shear rate was accompanied by an edge instability, however. Figure 2 shows a sequence of photographs of the edge during a single transient at 2500 Pa, using for this single run (to enable easier viewing) a lower plate without temperature control in place of the Peltier plate. The pictures, in sequence, are (a) after loading, (b) during the initial portion of the transient, (c) during the final portion of the transient, and (d) following careful removal of the material that had been extruded during the transient from the exterior of the fixture. About 0.08 g of extruded material, comprising about 14% of the total volume, was collected. Loss of material from the fixture is clearly seen in Figure 2d, from which we estimate a reduction in the radial contact of about 1.8−1.9 mm, corresponding to a volume loss of about 25%.

Figure 3 shows an analogous series of creep tests carried out by first stepping up to 5500 Pa and then decreasing the input stress from 5500 to 500 Pa. As in the previous experiments, the sample was permitted to rest without stress for 5 min between runs. Sample loss (not shown) occurred during the initial steps to the high stresses.

Figure 4 shows the magnitude of the complex modulus ($|G^*|$) before and after the onset of edge fracture;

† Present address: Kraft Foods, Glenview, IL 60025-4391.
* To whom correspondence should be addressed. E-mail: denn@ccny.cuny.edu.

10.1021/ma0510901 CCC: $30.25 © 2005 American Chemical Society
Published on Web 10/04/2005

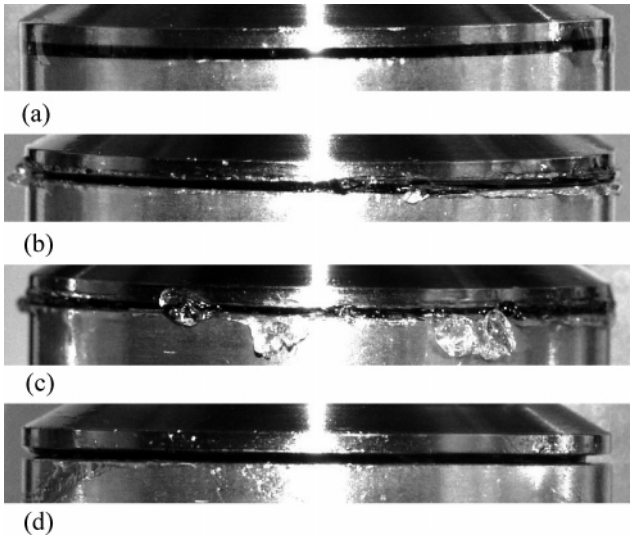

Figure 2. Pictures of the meniscus (a) after sample loading, (b) during the initial transient following step-up to 2500 Pa, (c) during the final portion of the transient, and (d) with extruded material removed from the exterior of the fixture. The pictures were taken without temperature control by the Peltier plate for better visualization of the meniscus shape.

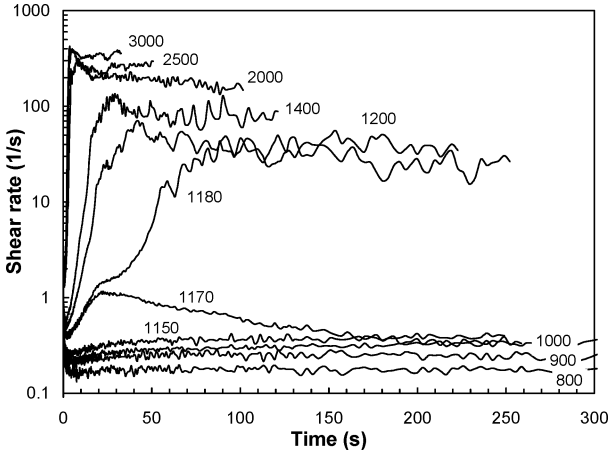

Figure 3. Shear rates as functions of time at constant input stresses from 5500 to 500 Pa. The sample was fully relaxed for 5 min after each creep experiment and then stepped up to the next stress.

the uniform decrease of about 30% at all frequencies following edge fracture is a consequence of the loss of material. The 30% decrease in $|G^*|$ is consistent with the estimate of a 25% volume loss from Figure 2d. The figure also shows the steady flow curve from ascending (Figure 1) and descending (Figure 3) creep tests that used different samples. The loss of material is reflected in the decreased stress at low rates in the two descending tests; the descending tests were done sequentially with the same sample. The fractional decrease in the steady stress below the plateau is comparable to the decrease in the magnitude of $|G^*|$ from the oscillatory experiments.

3. 7.5% Solution

The 7.5% solution provided by Professor Wang shows essentially the same behavior, but it is easier to work with and thus somewhat more revealing. Figure 5 shows the results of creep experiments at constant nominal stresses ranging from 500 to 3000 Pa, which should be compared to Figure 6a in Tapadia and Wang[1] and to

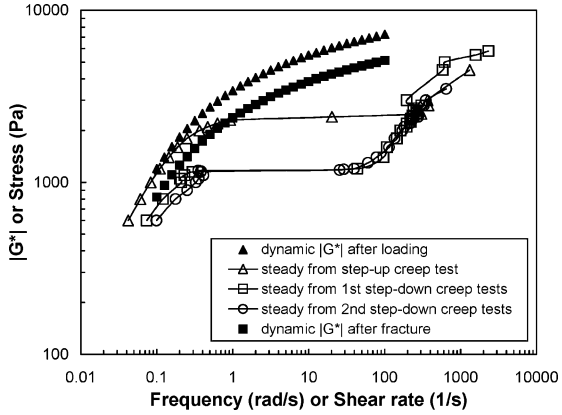

Figure 4. Magnitude of the complex modulus ($|G^*|$) as a function of frequency after sample loading (filled triangles) and following edge fracture (filled squares), together with the steady-state flow curve (applied shear stress as a function of steady shear rate) from the ascending creep data in Figure 1 (open triangles), the descending creep data in Figure 3 (open squares), and a second sequence of descending creep data (open circles).

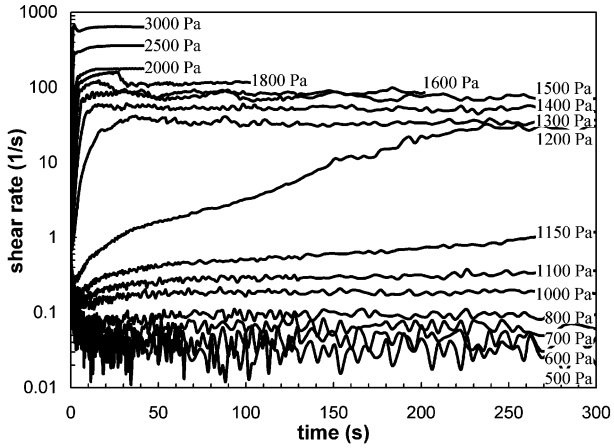

Figure 5. Shear rates as functions of time for the 7.5% solution at constant input stresses from 500 to 3000 Pa. The sample was fully relaxed for 5 min after each creep experiment and then stepped up to the next stress.

Figure 1 above. The sample was permitted to relax without stress for 5 min after each measurement and then stepped up to the designated stress, starting at 500 Pa and increasing to 3000 Pa. The shape change between 1150 and 1300 Pa, with an increase in shear rate of more than an order of magnitude, and the long, slow transient at 1200 Pa, with an apparent shoulder at about 50 s, are analogous to the transition observed by Tapadia and Wang in the 10% solution between 2000 and 3000 Pa and the transient at 2500 Pa, which are also seen here in Figure 1. The long transient in shear rate was accompanied by an edge instability. Parts a and b of Figure 6 show the shape of the meniscus after loading the sample and following development of the severe edge instability at 1200 Pa, respectively. The edge fracture did not appear to propagate inward with increasing shear stress for this sample and seemed instead to stabilize. The tacky material that rolled out from the cone-and-plate fixture spread around the rim with continuing steady shear, creating the visual impression of a smooth edge, as shown in Figure 6c. In one trial we attempted to recover the material that had been extruded during the transient. The sample was too tacky for us to recover all of the extruded material, but about 0.04 g, comprising about 7.5% of total volume, was

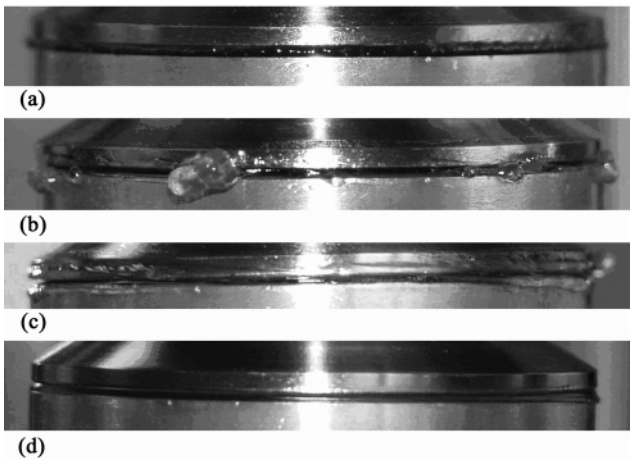

Figure 6. Pictures of the meniscus of the 7.5% solution (a) after sample loading, (b) with maximum edge fracture following step-up to 1200 Pa, (c) with stabilized maximum edge fracture by continuing rotation of the cone, and (d) with minimum edge fracture following step-up to 3000 Pa. The pictures were taken without temperature control by the Peltier plate for better visualization of the meniscus shape.

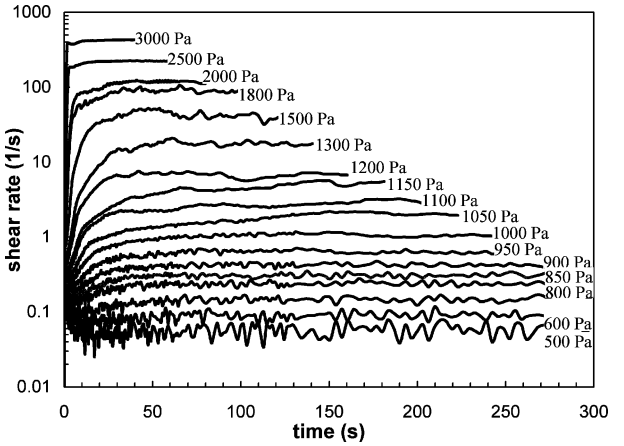

Figure 7. Shear rates as functions of time at constant input stresses from 3500 to 500 Pa. The sample was fully relaxed for 5 min after each creep experiment and then stepped up to the next stress.

collected. The loss of material can be seen clearly on the left side of Figure 6c, from which we estimate a reduction in the radial contact of about 1.1 mm; this corresponds to a volume loss of about 15%.

The edge instability appeared to be less severe at high stresses. Thus, we carried out an analogous series of creep tests by first stepping up to 3000 Pa and then decreasing the input stress from 3000 to 500 Pa, as shown in Figure 7. The meniscus following a stress jump from rest to 3000 Pa is shown in Figure 6d. As in the previous experiments, the sample was permitted to rest without stress for 5 min between runs. A long transient in shear rate and a shape transition in the shear rate curve were not observed at any stress level. The extent of edge fracture gradually increased with decreasing stress, but the shape of the meniscus always stabilized quickly, and there was less material loss than in the creep experiments that ascended through the plateau.

The magnitudes of the complex modulus measured in oscillatory shear after sample loading, after maximum edge fracture (stress jump to 1200 Pa), and after minimum edge fracture (stress jump to 3000 Pa) are compared in Figure 8, both in absolute terms and as

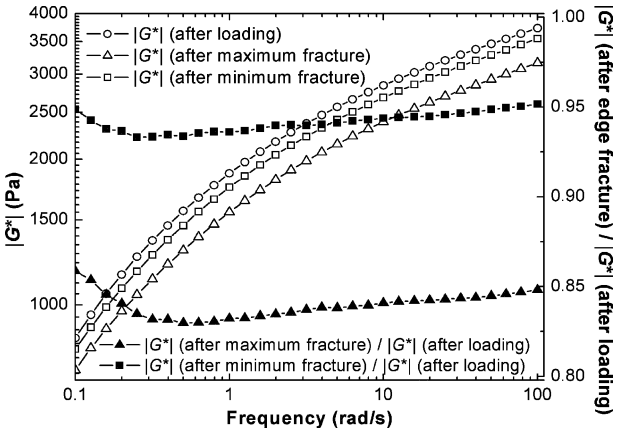

Figure 8. Magnitude of the complex modulus ($|G^*|$) as a function of frequency after sample loading (open circles), maximum edge fracture (open triangles), and minimum edge fracture (open squares). The ratio of $|G^*|$ after maximum edge fracture (filled triangles) and minimum edge fracture (filled squares) to $|G^*|$ after sample loading is also shown.

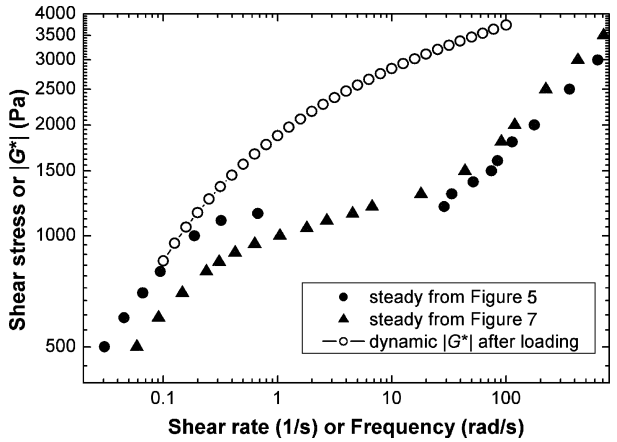

Figure 9. Steady-state flow curve (applied shear stress as a function of steady shear rate) from the creep data in Figure 5 (filled circles) and Figure 7 (filled triangles), together with $|G^*|$ after sample loading (open circles) as a function of frequency.

ratios. The magnitude of $|G^*|$ decreased almost uniformly by 15% and 5% after the maximum and minimum edge fracture, respectively. The 15% decrease after maximum edge fracture is consistent with the visual estimate of material loss from Figure 6c.

Steady-shear flow curves (filled symbols) are shown in Figure 9. These were obtained from the steady-state values in the creep experiments shown in Figures 5 and 7. The steady-state flow curve obtained from the data in Figure 5 (filled circles) exhibits a discontinuity of more than an order of magnitude, much like that shown in Figures 7 and 8 of Tapadia and Wang.[1] (The corresponding curve in our Figure 4 contains one intermediate point.) The steady-state flow curve obtained from the data in Figure 7 (filled triangle), however, is continuous, although it is clear from the oscillatory measurements and the low-rate data that it is displaced vertically from the correct flow curve by about 5% because of a small amount of material loss following the first stress jump.

The continuous flow curve is shown shifted vertically in Figure 10 to compensate for the reduced contact area, together with the low-rate data from the creep experiments in Figure 5 and the oscillatory data obtained after loading. The same shift factor was used at all frequencies, which assumes equal contact area for all points.

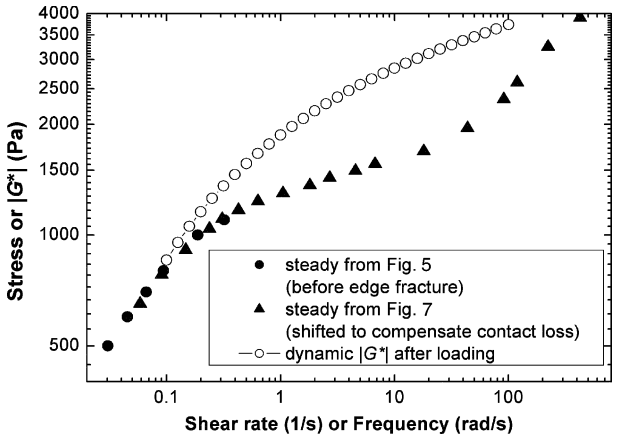

Figure 10. Steady-state flow curve from Figure 7 shifted vertically (filled triangles), together with the steady-state flow curve from Figure 5 below 1200 Pa (filled circles) and $|G^*|$ after sample loading (open circles) as a function of frequency.

4. Discussion

The steady-shear data in Figure 10 show the usual terminal, plateau, and transitional regimes observed with highly entangled solutions of narrow-distribution polymers using controlled-displacement rheometers when the shear is applied for only a short period to prevent the onset of edge fracture,[1,3,4] and the data appear to be at least qualitatively consistent with the predictions of modern molecular theories of entangled polymers. There is no evidence of yieldlike behavior and an "entanglement−disentanglement transition" as posited by Tapadia and Wang.[1,2] Furthermore, the observations do not support Tapadia and Wang's contention that reliable data can be obtained only with a torque-controlled rheometer. Indeed, it is important to note that the mechanical input to a torque-controlled rheometer is torque, hence average stress, and that there is no guarantee of a uniform stress field within the fixture.

"Runaway" is the inevitable consequence of a loss of material in a region where the slope of the stress curve is very small. The slope of the steady flow curve in Figures 9 and 10 in the power-law region for the 7.5% solution is about 0.085, for example. The shear-rate ratio at steady state before and after the loss of material at constant torque equals the ratio of wetted radii raised to the power $3/n$, or ~35; the loss of 1.1 mm of surface contact, which is the amount of material loss estimated from Figure 6d, would therefore correspond to an 8-fold increase in shear rate at steady state. The actual increase, as shown in Figure 9, is more than 30-fold, but the calculation is very sensitive to the value of n and the radius ratio, neither of which is known accurately. In addition, the calculation does not take into account any transient temperature increase caused by the rapid increase in shear rate during apparent "runaway", which would tend to lower the viscosity even more. The slope in the plateau region for the 10% solution in Figure 4 is 1 order of magnitude smaller, and the calculation predicts an unrealistic jump of 10^{12} because of the loss of material, or total runaway, but this slope is too unreliable for any useful deduction.

We have no explanation for the marked difference in edge fracture in the 7.5% sample before and after the plateau, other than that the small amount of material loss following the initial stress jump to 3000 Pa appears to be sufficient to constrain the edge instability to within the fixtures in the neighborhood of the plateau for this sample, which is not the case for the 10% sample with the somewhat smaller polydispersity.

References and Notes

(1) Tapadia, P.; Wang, S. Q. *Macromolecules* **2004**, *37*, 9083.
(2) Tapadia, P.; Wang, S. Q. *Phys. Rev. Lett.* **2003**, *91*, 198301.
(3) Pattamaprom, C.; Larson, R. G. *Macromolecules* **2001**, *34*, 5229.
(4) Bercea, M.; Peiti, C.; Simionescu, B.; Navard, P. *Macromolecules* **1993**, *26*, 7095.

MA0510901